RESEARCH

The anomalously hot summer of 2021 over the Euro-Mediterranean region: underlying atmospheric drivers and heatwaves

Meral Demirtaş[1]

Abstract

This study investigated the atmospheric drivers and heatwave diagnostics of June to August (JJA) 2021 period over the Euro-Mediterranean region. Analyses of seasonal and monthly anomaly of geopotential height at 500 hPa (GH500) indicated that heatwaves were collocated with upper-level atmospheric anomalies. In June, the panoply of large-scale atmospheric flow resembled a ridge-trough-ridge wave train. A prominent ridge structure was noted over south-eastern Europe. This area was also marked with positive GH500 anomaly which extended all the way from north-western Europe to southern Europe. In July, the upper-level flow was zonal over western Europe, but meridional over eastern Mediterranean. Western Europe exhibited negative GH500 anomalies, while eastern Mediterranean had positive GH500 anomalies. In August, the upper-level flow exhibited quasi-zonal flow. North-eastern and south-eastern Europe exhibited higher GH500 than climate mean (1980–2009), while north-western Europe had lower GH500. Both the Mediterranean Sea and the Black Sea had approximately + 3 °C above climate averages in July and August. The total number of heatwave days varied from 5 to 45 days for JJA. In June, some parts of south-eastern Europe and eastern Turkey had approximately 3–18 heatwave days; duration of heatwaves varied from 3 to 15 days in July; they were located over south-eastern Spain, southern Italy, eastern Europe and Turkey; in August, heatwaves lasted much longer compared to June and July over southern parts of Spain and Italy, the Balkan peninsula and Turkey which ranged from 3 to 30 days. Heatwave events of July and August were related to the atmospheric blocking events.

1 Introduction

The frequency and intensity of heatwaves may change in response to shifts in both climate mean and climate variability. The year of 2021 was expected to be less warm due to the cooling of effects of the 2020–2022 La Niña events, but on the contrary, it was listed among the seven warmest years (2015–2021) on record by the World Meteorological Organization (WMO 2022). According WMO records, among the seven consecutive warmest years, 2016, 2019 and 2020 are at the top three. The 2021 was considered to be the fifth warmest year on record (Copernicus Climate Change Service 2021). Being 1.11 °C higher than the pre-industrial (1850–1900) climate average, the global mean temperature of 2021 is near to the lower limit of global temperature increase of the Paris Agreement, which is 1.5 °C.

Europe had its second-warmest July on record, with several parts of southern Europe exceeding surface temperatures being higher than 40 °C (Copernicus Climate Change Service 2021). Over the Mediterranean region, extremely hot weather affected many countries. On 20 July, Cizre with 49.1 °C set a Turkish national record (WMO 2022). On 11 August, in Sicily in Italy, surface temperatures were 48.8 °C. On 14 August, Montoro, the surface temperature of 47.4 °C set a national record for Spain, whilst Madrid had its recorded hottest day with 42.7 °C (WMO 2022).

Major forest fires took place across various parts of southern Turkey and Greece, which lasted several days (JRC 2021). From 28 July to 12 August, massive and destructive wildfires took place across parts of south-western Turkey (Telegraph 2021, Sabah 2021). On 28 August 2021, the wildfires with huge smoke clouds happened in Manavgat town of Antalya, and it stretched over Muğla and its provinces, such as Bodrum and Marmaris. On the Aegean coast, tourists were evacuated from Bodrum. More than 200 wildfires took place on the south-western coastline of Turkey (JRC 2021; Anadolu Agency 2021). The wildfires burned

✉ Meral Demirtaş
meral.demirtas@samsun.edu.tr

1 Department of Meteorology, University of Samsun, Samsun, Turkey

out 206,000 ha, eight people died, including two firefighters, and approximately 3000 animals perished (JRC 2021; CNN 2021). In Greece, the west-central parts of Rhodes Island suffered from an extreme drought, and consequently, the wildfire affected the Valley of Butterflies, near the town of Tholos (JRC 2021). Destructive wildfires affected Catania in Sicily, Italy. Many residential places were damaged or burned out, with hundreds of people being evacuated (JRC 2021).

The relationship between the extremely hot temperatures and quasi-stationary high pressure systems are important for both in extreme weather events and in the analysis of heatwaves in the context of seasonal variability and climate change. Various climate scenarios project intense, more frequent and long-lasting hot spells (Zittis et al. 2021; Cherif et al. 2020; Hochman et al. 2020; García-León et al. 2021; Mbokodo et al. 2020; Domeisen et al. 2023). Heatwaves are usually related with the underlying atmospheric flow pattern and climatological anomalies. They are generally associated with quasi-stationary anticyclones which are also referred as blocking highs (Ionita et al. 2021; Demirtaş 2022; Demirtaş 2018; Schaller et al. 2018); they are characterised by downward motion, due to clear air conditions positive radiation anomalies, adiabatic warming and advection of warm air (Black et al. 2004; Baldi et al. 2006). Therefore, they are usually the main drivers of extremely high surface temperatures. Blocking highs are long-lasting atmospheric structures with a pronounced meridional flow component (Pfahl 2014; Schwierz et al. 2004). Hence, the prominent westerly zonal flow at mid-latitudes may be halted or diverted (Demirtaş, 2018; Pfahl, 2014). Blocking highs may vertically cover the whole troposphere (Schwierz et al. 2004). Blocking can lead to extremely hot or cold surface temperatures depending on the season (Quandt et al. 2017), extremely dry or wet hydrological conditions (Lenggenhager et al. 2019), heatwaves (Rodrigues et al. 2019; Demirtaş 2018; Demirtaş 2017b), cold snaps (Pfahl and Wernli 2012; Demirtaş 2022; Demirtaş 2017a) and poor air quality (Webber et al. 2017).

Previous studies reported that anomalous sea-surface temperatures (SST) may also maintain and enhance prolonged heatwaves (Di Capua et al. 2021; Feudale and Shukla 2007, 2011; Xoplaki et al. 2003). It should also be noted that both the Mediterranean Sea and the Black Sea had approximately + 3 °C above climate averages (1979–2000) in July and in August in 2021 (not shown in here) (Climate Reanalyzer 2022).

The main objectives of this study are (i) to examine the summer of 2021 with a focus on temperature extremes in the light of underlying atmospheric conditions, (ii) to detect heatwave events with an objective heatwave detection method and (iii) to diagnose presence of atmospheric blocking events and their association with heatwave events.

This article is organised as follows: Section 2 presents methodologies used for diagnosing heatwaves and atmospheric blocking events. Section 3 gives results of heatwave events and blocking analysis. Section 4 summarises the key findings and presents concluding remarks.

2 Methods

The anomalously hot summer of 2021 of the southern Europe will be addressed with a focus on the role played by the upper-level atmospheric dynamics by using the period mean of the 500-hPa geopotential heights and their differentials from the base climate (1980–2009). Since heatwaves are closely related with blocking, this study uses a two-dimensional blocking index to detect the existence of blocking. Detection of heatwaves will be performed by using a non-parametric objective method, which employs spatially and temporally varying temperature thresholds.

2.1 Atmospheric data

The European Centre for Medium-Range Weather Forecasts (ECMWF) reanalysis data (ERA5) (Hersbach et al. 2020) is employed in this study. The geopotential height at 500 hPa (Z500) is used for the blocking index, and temperature at 2 m (T2m) is used for heatwave diagnostics.

The following is computed for the study period (1 June–31 August 2021) in order to analyse the hot spells of summer 2021: (i) the period mean of 500-hPa geopotential height (GH500); (ii) GH500 anomalies are computed from the difference between the temporal mean of the 1 June–31 August 2021 and the 1980–2009 climatological mean; (iii) the period mean of 2-m surface temperature (T2m); and (iv) T2m anomalies are determined from the difference between the temporal mean of the study period and the climatological mean of 1980–2009 period.

2.2 Detection of Blocking

The detection of atmospheric blocking is conducted with a two-dimensional blocking index (Demirtaş 2018). The 2D blocking index uses GH500 as introduced by Tibaldi and Molteni (1990), and it is elaborated to include variations in zonal and in meridional directions (Davini et al. 2021; Scherrer et al. 2006). In order to elucidate it further, some spatiotemporal metrics were also implemented (Davini et al. 2021; Demirtaş 2022). Using GH500 from 30°N to 80°N, I calculated southern and northern geopotential height gradients (SG and NG respectively) for the 45°N–75°N latitudes. Blocking is a large-scale atmospheric pattern in which a quasi-stationary anticyclone halts or diverts the prominent westerly flow at mid-latitudes (Rex 1950; Tibaldi and Molteni 1990;

Brunner et al. 2018a); accordingly in this research, highs to the north of 45°N latitude are considered (Davini et al. 2021; Brunner et al. 2018b). The 2D index required SG and NG is computed as follows:

$$SG(\lambda_0, \Phi_0) = \frac{Z_{500}(\lambda_0, \Phi_0) - Z_{500}(\lambda_0, \Phi_S)}{\Phi_0 - \Phi_S} \quad (1)$$

$$NG(\lambda_0, \Phi_0) = \frac{Z_{500}(\lambda_0, \Phi_N) - Z_{500}(\lambda_0, \Phi_0)}{\Phi_N - \Phi_0} \quad (2)$$

where λ represents a longitude and Φ is used for a latitude, and 0 denotes a starting latitude or longitude, while S and N denote south and north respectively. At each grid point, the below given criteria for SG and NG are used respectively (Tibaldi and Molteni 1990):

$$SG(\lambda_0, \Phi_0) > 0 \quad (3)$$

$$NG(\lambda_0, \Phi_0) < -10 \text{m/}°\text{latitude} \quad (4)$$

The criterion defined in Eq. 7 represents the reversal of the gradient of Z500 with easterlies south of a related latitude (Φ). The criterion given in Eq. 4 (NG < − 10 m/° latitude) shows westerlies to the north of a related latitude (Φ) (Tibaldi and Molteni 1990).

An instant blocking event is assigned at a given grid point, when conditions presented in (3) and (4) are concurrently met. Large-scale sectoral blocking is determined, when the metrics defined in (3) and (4) are met for at least 15 longitudes. A temporal scale of 5 days is applied for diagnosing an episode of blocking. A blocking event is assigned as large-scale episode blocking, when spatial and temporal criteria are both fulfilled.

2.3 Non-parametric heatwave method and its metrics

Spatiotemporal diagnostics of the heatwaves of June–July–August (JJA) 2021 were performed by using a non-parametric approach to determine a spatiotemporally changing maximum temperature threshold, which is a 90th percentile (T2mP90) from a 7-day temporal period (Demirtaş 2022). This threshold is computed for each respective calendar day (RCD) as the 90th percentile of the climatological distribution of daily maximum temperature at a grid point in one of the two temporal periods with a ± 3-day window centred on each side of the RCD, and then assigned as the maximum threshold temperature.

where both $\bigcup$ is used for showing the union of T2m; the first one is for the reference climatology period and the second one is for the two time windows of the RCD. In above, $\text{T2m}_{(\text{latitude, longitude, year, day})}$ represents the maximum T2m and $\text{T2mP90}_{(\text{latitude, longitude, RCD})}$ represents the 90th percentile maximum temperature threshold of the RCD. An illustrative example may be given in here; T2mP90 of 12 July is determined by considering maximum temperatures from 9 July to 15 July of the base climate period.

Two criteria are applied for assigning a heatwave: (1) the first criterion is the T2m of an RCD must be equal or higher than the calculated T2mP90 and (2) the second criterion is the satisfaction of the first criterion for three uninterrupted days. Then, a heatwave event (HWE) is assigned to the grid-point if metrics defined in (1) and (2) are both concurrently fulfilled. Accordingly, HWE is assigned to 1, otherwise to 0. Thus, HWE = 1 means a heatwave event took place, and HWE = 0 means there is no heatwave event.

3 Results

3.1 An overview of period mean and climatological anomalies

June-July-August (JJA) 2021 period mean of GH500 is presented in Fig. 1a, and their differentials from the base climate are given in Fig. 2a. The mean zonal flow dominated over the Euro-Mediterranean region (Fig. 1a). In order to analyse the underlying atmospheric situation in detail, each month was examined separately. In June, the panoply of large-scale atmospheric flow resembled a ridge-trough-ridge wave train (Fig. 1b). A prominent ridge structure was noted over the south-eastern Europe. This area was also marked with a GH500 anomaly which extended all the way from the north-western Europe to the southern Europe (Fig. 2b). In July, the upper-level flow was zonal over the western Europe, and meridional over the eastern Mediterranean (Fig. 1c). In terms of underlying GH500 anomalies, the western Europe exhibited negative anomalies, while the eastern Mediterranean region had positive anomalies (Fig. 2c). In August, the upper-level flow exhibited quasi-zonal flow throughout the study region (Fig. 1d). Comparing August 2021 GH500 period mean with the base climate (1980–2009) indicated that the north-eastern and the south-eastern Europe exhibited GH500 values larger than that of climate mean, while the north-western Europe had lower than climate mean (Fig. 2b).

The horizontal distribution of the JJA 2021 period-mean T2m showed that warm places with T2m varying

$$\text{T2mP90}_{(\text{latitude, longitude, RCD})} = \bigcup_{y=1980}^{2009} \bigcup_{t=\text{RCD}-3}^{\text{RCD}+3} \text{T2m}_{(\text{latitude, longitude, year, day})}$$
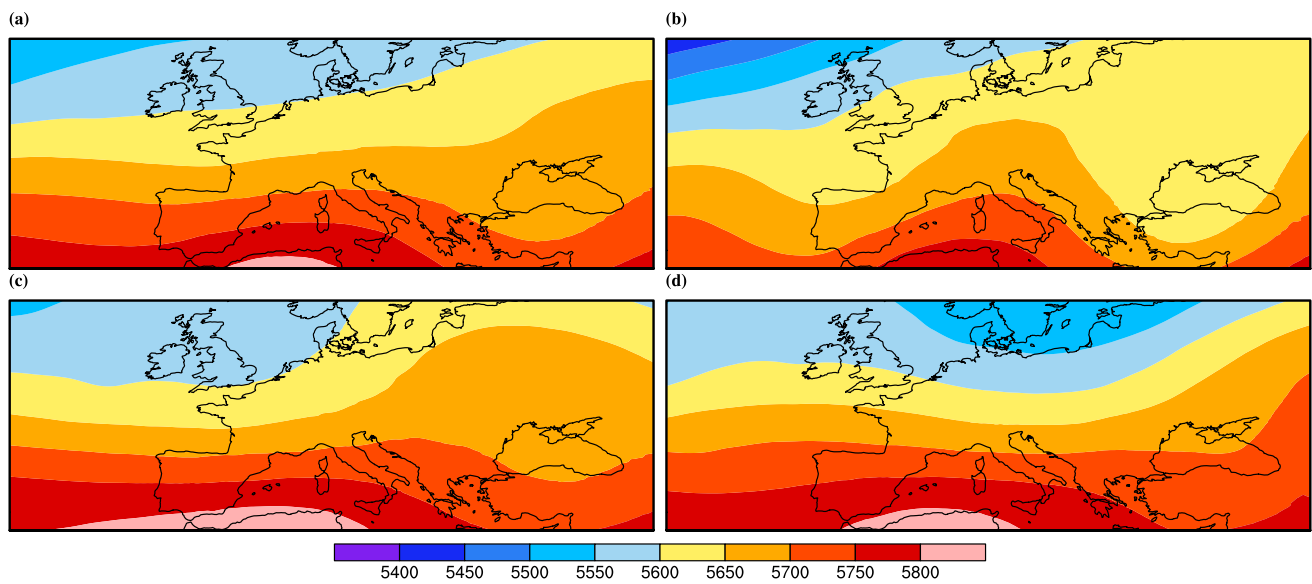
Fig. 1 The period mean of GH500 (in gpm): **a** June-July-August 2021; **b** June 2021; **c** July 2021; and **d** August 2021
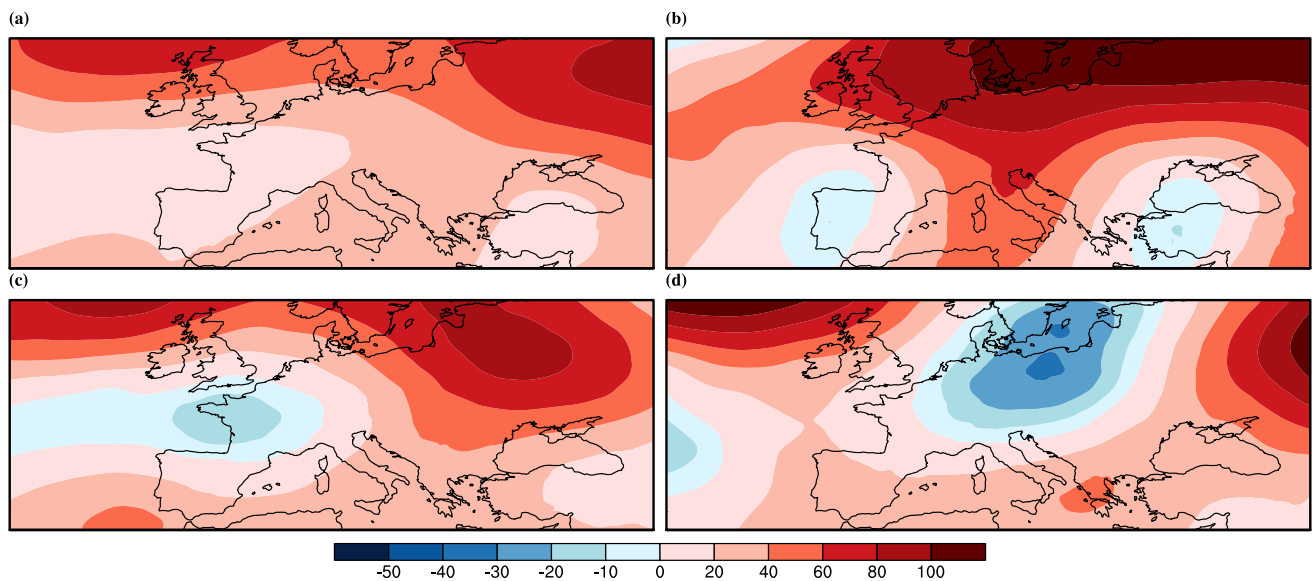

Fig. 2 The anomaly of GH500 (in gpm) with respect to the base climate (1980–2009): **a** June-July-August 2021; **b** June 2021; **c** July 2021; and **d** August 2021

from 30 to 35 °C were situated over some parts of the Euro-Mediterranean region, including Spain, Italy, the eastern Europe and Turkey (Fig. 3a). How these period-mean T2m values translated into climatological anomalies were examined by considering differentials of them with the base climate (1980–2009). The T2m anomalies of JJA period varied from 6 to 10 °C over the south-eastern Europe and Turkey (Fig. 4a). Examination of each month showed that in June, the southern parts of Spain and France, the south-eastern Italy, the eastern Europe and the western and

southern parts of Turkey exhibited higher temperatures (Fig. 3b). T2m anomaly of June varied from 8 to 12 °C, and it extended from the north-eastern Europe to the southern Europe and the eastern Turkey (Fig. 4b); the T2m anomaly was collocated with the GH500 positive anomaly (Fig. 2b). In July, very hot conditions were noted over the most of the Euro-Mediterranean region; T2m values ranged from 25 to 35 °C (Fig. 3c). In this research, grid-based (in 0.25° × 0.25° horizontal resolution) surface temperatures were averaged over the study period. It should be emphasised that
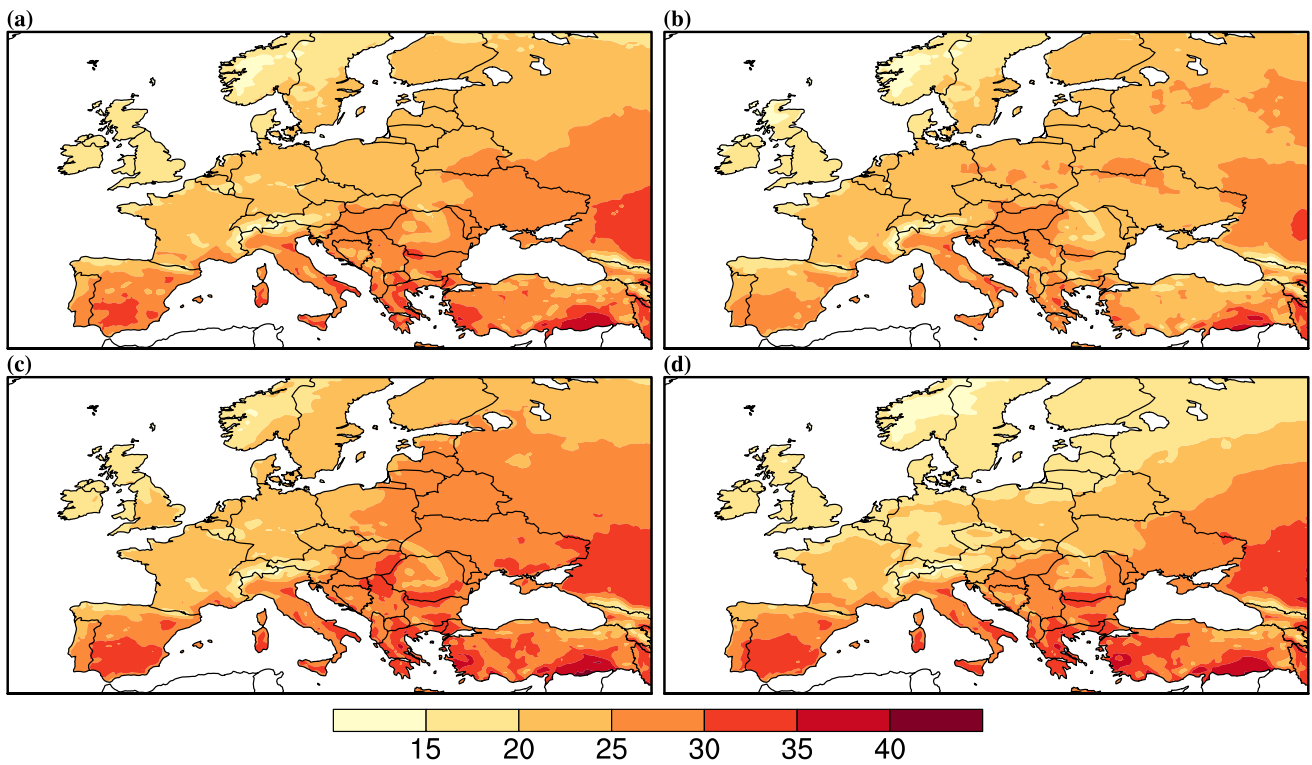
Fig. 3 The period time mean of T2m (in degC): **a** June-July-August 2021; **b** June 2021; **c** July 2021; and **d** August 2021
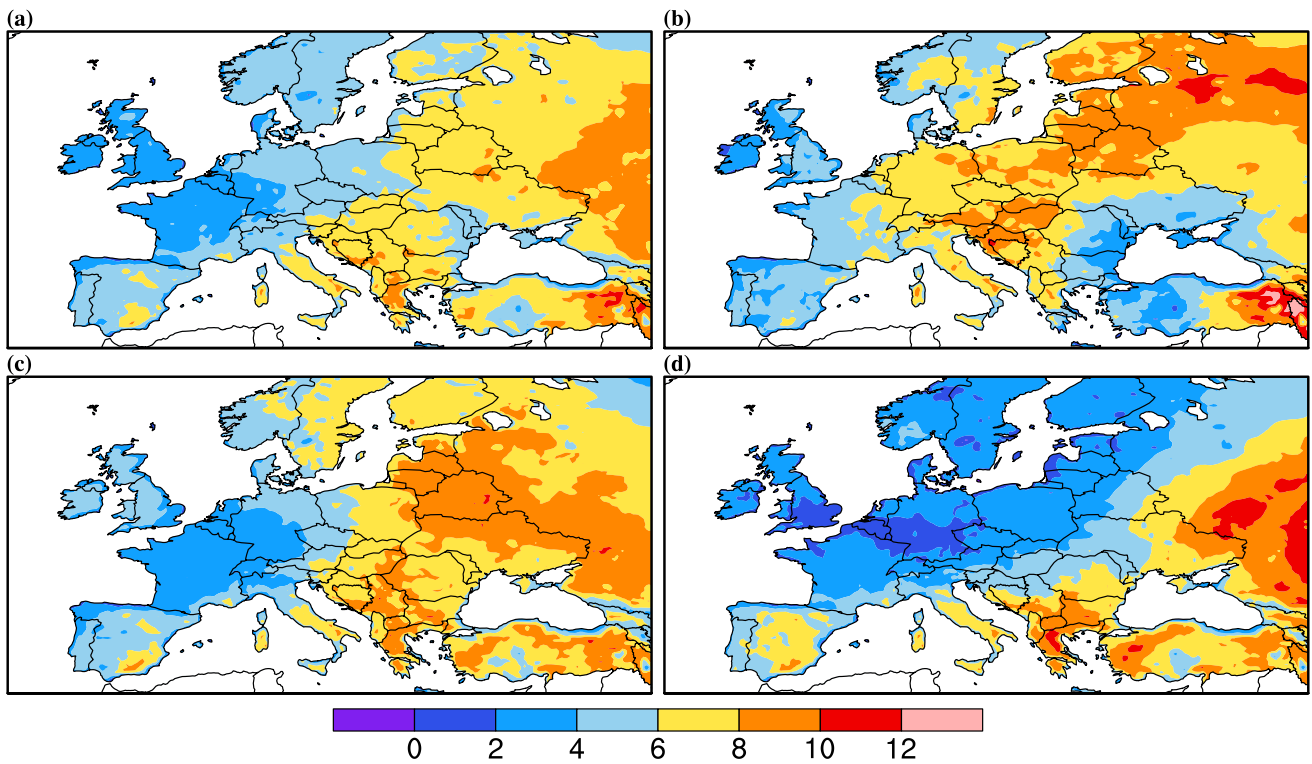

Fig. 4 The anomaly of T2m (in degC) with respect to the base climate (1980–2009): **a** June-July-August 2021; **b** June 2021; **c** July 2021; and **d** August 2021

station-point daily observed temperatures are much higher with respect to spatiotemporally averaged temperatures shown in here (WMO 2022). The underlying climatological anomalies varied from 6 to 10 °C over the south-eastern Spain, south-eastern Italy and the north-eastern and south-eastern Europe and Turkey (Fig. 4c). In August, the Euro-Mediterranean region and Turkey experience high temperatures ranging from 25 to 35 °C (Fig. 3d). Comparing August 2021, mean T2m values with the reference climate period (1980–2009) showed that some parts of Spain, Italy, the Balkan peninsula and north-east of Turkey exhibited T2m climatological anomalies varying from 6 to10 °C (Fig. 4d), where the GH500 positive anomalies of August were also collocated over the same area (Fig. 2d).

3.2 Summer heatwave analysis of 2021

Heatwave method given in Section 2.3 is used for examining the summer heatwaves of 2021. The 90th percentile-based temperature threshold varies spatially and daily, and therefore, it is compatible with microclimatic conditions of the study area. Analysis of the total number of heatwave days of JJA 2021 showed that the south-eastern part of Spain and the southern Italy Europe, the Balkan peninsula and some parts of Turkey were under hot summer conditions for approximately 5–45 days (Fig. 5a). Examining each month individually provides detailed account of each month. In June, some parts of south-eastern Europe and the eastern Turkey had approximately 3–18 heatwave days (Fig. 5b). It should be noted that some of these places collocated with the GH500 anomalies (Fig. 2b) and with the T2m anomalies (Fig. 4b). Duration of heatwaves varied from 3 to 15 days in July. Long-lasting heatwaves were located over the south-eastern Spain which were approximately 15–20

days (Fig. 5c), while the southern Italy had 10–12-day long heatwaves. The western parts of Greece and the south-western and eastern parts of Turkey experienced 12–18-day heatwaves (Fig. 5c). In August, heatwaves lasted much longer compared to June and July, in particular over southern parts of Spain and Italy, the Balkan peninsula and north-east of Turkey, which ranged from 3 to 30 days (Fig. 5d). This highly affected region was coincided with the high GH500 anomaly (Fig. 2d) and the large T2m anomaly (Fig. 4d).

During the JJA 2021 period, the total number of heatwaves varied from 1 to 7. The total number of heatwaves were especially large over the eastern Spain, the southern Italy, the south-eastern Europe, the Balkan peninsula and the south-western and the eastern parts of Turkey (Fig. 6a). Examination of each month separately indicated that the eastern Europe had 1–2 heatwave events in June (Fig. 6b). In July, the eastern Europe and Turkey had more heatwaves which ranged from 1 to 3 events (Fig. 6c). In August, the northern Spain, the southern Italy, the south-eastern Europe and the western Turkey had various heatwaves which ranged from 1 to 4 (Fig. 6d). These heatwave intense regions of August 2021 collocated with the GH500 positive anomalies (Fig. 2d) and the largest T2m anomalies (Fig. 4d).

3.3 Role of upstream atmospheric blocking

Hot spells are generally associated with atmospheric blocking (Schaller et al. 2018; Demirtaş 2022, Demirtaş 2018, Demirtaş 2017b). In order to elucidate this, the blocking detection method is used for examining the JJA of 2021. There were approximately 6–28 days of total number of instantaneous blocking over the northern latitudes (Fig. 7a). In June, there were 4–14 days of instantaneous blocking (Fig. 7b). Instantaneous blocking over the northern
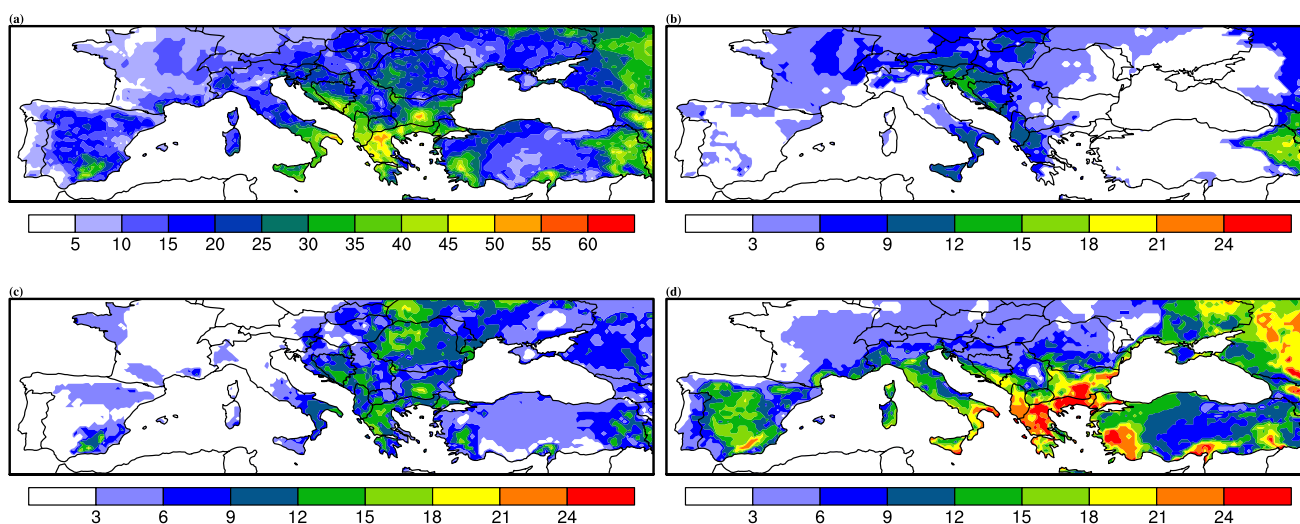

Fig. 5 Horizontal distributions of total number of heatwave days: **a** June-July-August 2021; **b** June 2021; **c** July 2021; and **d** August 2021
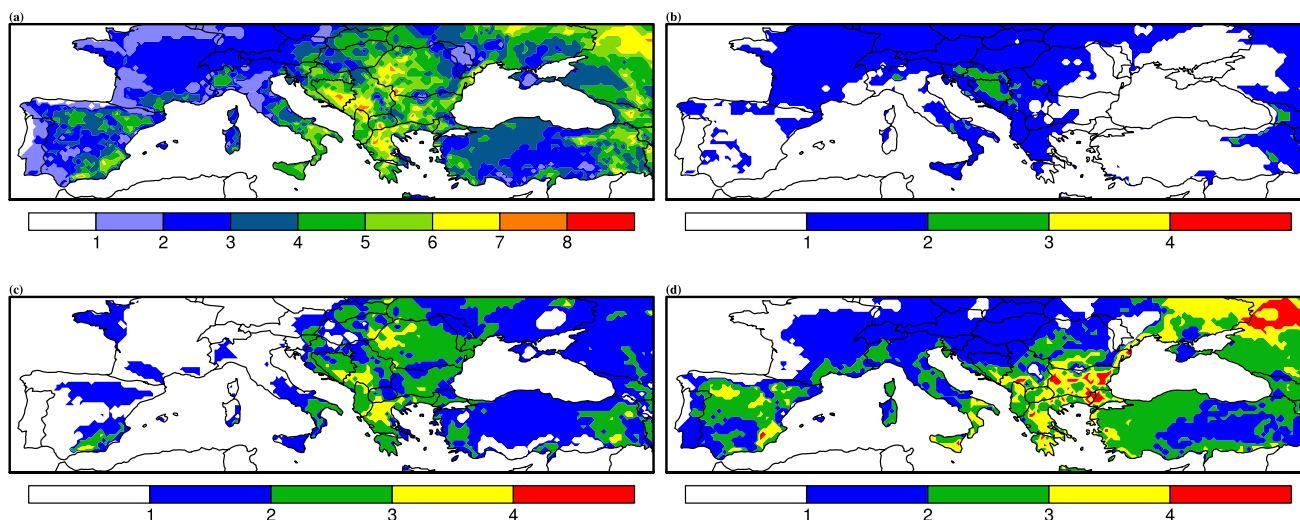
Fig. 6 Horizontal distributions of total number of heatwaves: **a** June-July-August 2021; **b** June 2021; **c** July 2021; and **d** August 2021

latitudes lasted 2–6 days in July (Fig. 7c). In August, there were two main blocking regions over the northern latitudes (Fig. 7d); the one over the north-west had 2–4 days, while the one over the north-east had 2–14 days, which collocated with some parts of the GH500 anomaly of the August 2021 (Fig. 2d).

The total number of large-scale episode of blocking is subjected to temporal and spatial metrics, and therefore, the total number of blocking events is quite different from the results of instantaneous blocking. Analysis of the results of total number of large-scale episode of blocking for JJA

2021 indicated that there were approximately 5–15 days of blocking over the north-east of the study region (Fig. 8a). Examination of each month's large-scale episode of blocking showed that blocked days ranged from 5 to 10 days over the north-eastern part of the study region in June (Fig. 8b). In July, there were approximately 6–10 large-scale episode of blocking on the north-east of the study area (Fig. 8c), which was coincided with the upper-level GH500 positive anomaly (Fig. 2c). In August, large-scale episode of blocking was noticeable over north-western and north-eastern parts of the study region which lasted for approximately 5–10 days
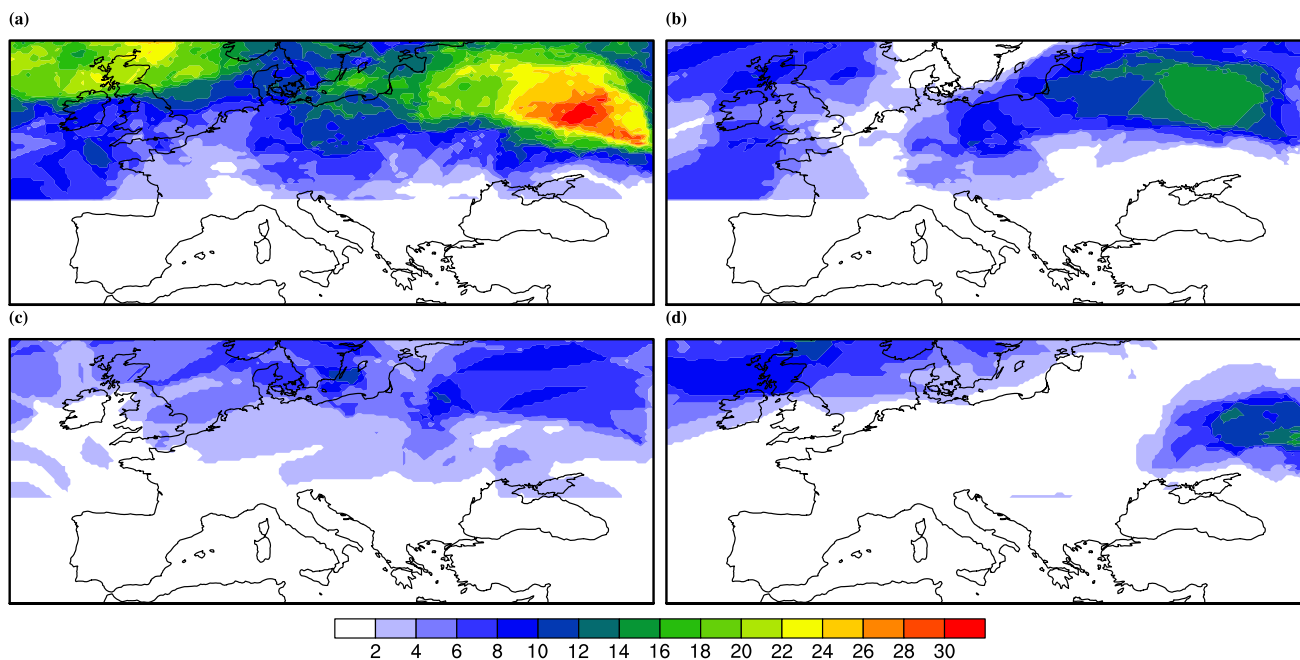

Fig. 7 Total number of instantaneous blocking days: **a** June-July-August 2021; **b** June 2021; **c** July 2021; and **d** August 2021
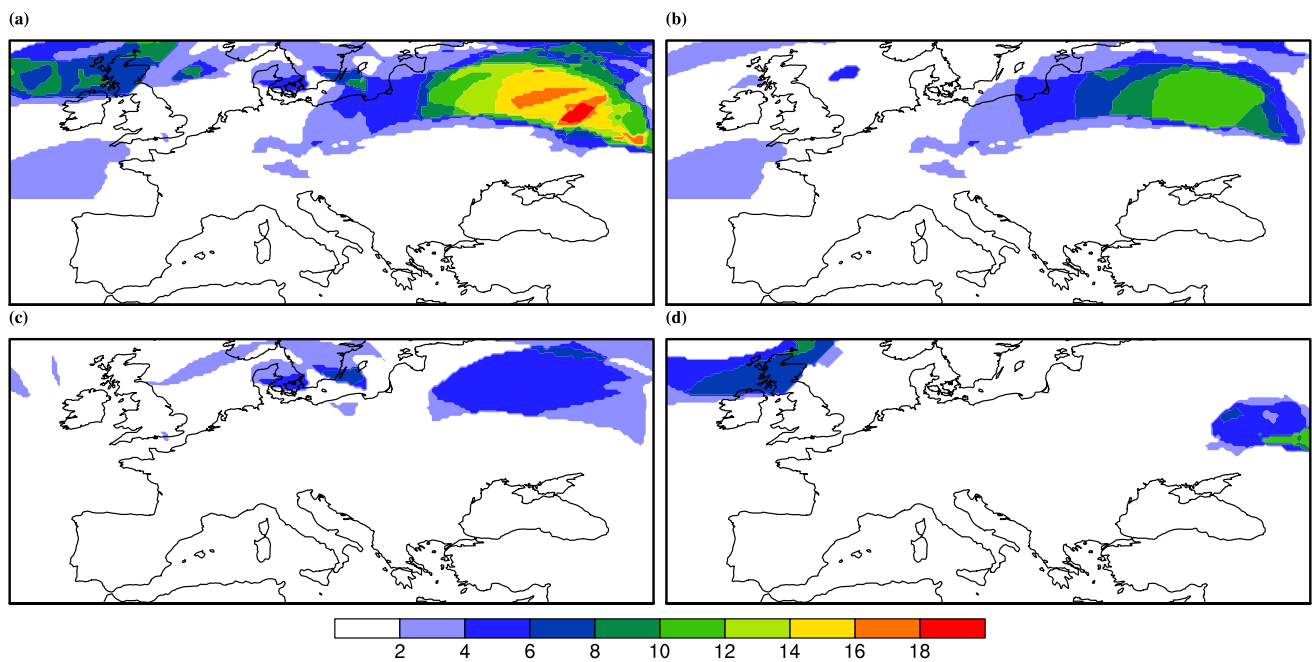
Fig. 8 Total number of large-scale episode of blocking days: **a** June-July-August 2021; **b** June 2021; **c** July 2021; and **d** August 2021

(Fig. 8d), which also collocated with some parts of GH500 anomaly (Fig. 2d), T2m anomaly (Fig. 4d), total number of heatwave days (Fig. 5d) and total number of heatwave events (Fig. 5d).

4 Summary and concluding remarks

This study examined the relationship between the anomalous temperatures of summer 2021 and the associated atmospheric conditions. The position of GH500 anomalies affects the magnitude and lifetime of heatwave events. Analyses of seasonal and monthly anomaly of GH500 indicated that the most pronounced heatwave events were collocated with these upper-level atmospheric anomalies. In June, the panoply of large-scale atmospheric flow resembled a ridge-trough-ridge wave train. A prominent ridge structure was noted over the south-eastern Europe. This area was also marked with the GH500 anomaly which extended all the way from the north-western Europe to the southern Europe. In July, the upper-level flow was zonal over the western Europe, and meridional over the eastern Mediterranean. In terms of underlying GH500 anomalies, the western Europe exhibited negative GH500 anomalies, while the eastern Mediterranean region had positive GH500 anomalies. In August, the upper-level flow exhibited quasi-zonal flow though out the study region. Comparing August 2021 GH500 period mean with the base climate (1980–2009) indicated that the north-eastern and the south-eastern Europe exhibited higher than climate mean

GH500, while the north-western Europe had lower than climate mean values. It should also be noted that both the Mediterranean Sea and the Black Sea had approximately + 3 °C above climate averages (1979–2000) in July and in August (not shown in here) (Climate Reanalyzer 2022).

I present underlying ingredients and key findings of summer 2021: (i) the total number of heatwave days varied from 5 to 45 days; (ii) in June, some parts of south-eastern Europe and the eastern Turkey had approximately 3–18 heatwave days; (iii) duration of heatwaves varied from 3 to 15 days in July, they were located over the south-eastern Spain, the southern Italy, the eastern Europe and Turkey; (iv) in August, heatwaves lasted much longer compared to June and July, in particular over southern parts of Spain and Italy, the Balkan peninsula and Turkey which ranged from 3 to 30 days; (v) analysis of the results of total number of large-scale episode of blocking for JJA 2021 showed that there were approximately 5–15 days of large-scale blocking. In June, blocking days ranged from 5 to 10 days. In July, there were 6–10 large-scale blocking events. In August, large-scale episode of blocking lasted 5–10 days. These blocking events happened near to the heatwave-affected region; and (vi) heatwave events of July and August might be attributable to blocking events.

Author contribution Meral Demirtaş: conceptualisation, research, methodology, figures, formal analysis and investigation, writing and editing

Data availability Meteorological data can be obtained from the European Centre for Medium-Range Weather Forecasts.

Code availability For plotting figures, National Center for Atmospheric Research (NCAR) Command Language (https://www.ncl.ucar.edu/) can be obtained from the NCAR.

Declarations

Ethics approval The author complies with the guidelines of the journal Theoretical and Applied Climatology.

Consent to participate The author agreed to be part of this research.

Consent for publication The author agreed to the publication of this research.

Conflict of interest The author declares no competing interests.

References

Anadolu Agency-AA (2021) 91 of 101 forest fires under control in Turkey: Minister. https://www.aa.com.tr/en/environment/91-of-101-forest-fires-under-control-in-turkey-minister/2320116 (Accessed 25 January 2023)

Baldi M, Dalu G, Maracchi G, Pasqui M, Cesarone F (2006) Heat waves in the Mediterranean: a local feature or a largerscale effect? Int J Climatol 26(11):1477–1487. https://doi.org/10.1002/joc.1389

Black E, Blackburn M, Harrison G, Hoskins B, Methven J (2004) Factors contributing to the summer 2003 European heatwave. Weather 59(8):217–223. https://doi.org/10.1256/wea.74.04

Brunner L, Schaller N, Anstey J, Sillmann J, Steiner AK (2018a) Dependence of present and future European temperature extremes on the location of atmospheric blocking. Geophys Res Lett 45:6311–6320. https://doi.org/10.1029/2018GL077837

Brunner L, Hegerl GC, Steiner AK (2018b) Connecting atmospheric blocking to European temperature extremes in Spring. J Clim 30:585–94

Cherif S, Doblas-Miranda E, Lionello P, Borrego C, Giorgi F, Iglesias A, Jebari S, Mahmoudi E, Moriondo M, Pringault O, Rilov G, Somot S, Tsikliras A, Vila M, Zittis G (2020) Drivers of change. In: climate and environmental change in the Mediterranean Basin—current situation and risks for the future. In: Cramer W, Guiot J, Marini K (eds) First Mediterranean Assessment Report. Union for the Mediterranean, Plan Bleu, UNEP/MAP, Marseille, p 128

Climate Reanalyzer (2022) Climate Change Institute, University of Maine, USA, https://ClimateReanalyzer.org (Accessed 4 April 2022)

CNN (2021) 'The animals are on fire,' say devastated farmers as wildfires sweep Turkey. https://edition.cnn.com/2021/07/31/world/turkey-wildfires-manavgat-six-dead-intl/index.html (Accessed 25 January 2023)

Copernicus Climate Change Service (2021) Second hottest July in Europe on record. https://climate.copernicus.eu/copernicus-second-hottest-july-europe-record (Accessed 4 April 2022)

Davini P, Weisheimer A, Balmaseda M, Johnson SJ, Molteni F, Roberts CD, Senan R, Stockdale TN (2021) The representation of winter Northern Hemisphere atmospheric blocking in the ECMWF seasonal prediction systems. Q J R Meteorol Soc:1344–1363

Demirtaş M (2017a) Intense heat waves: dynamical-physical factors and characteristics of these heat waves. (Şiddetli sıcak hava dalgaları: dinamik-fiziksel etkenler ve bu sıcak hava dalgalarının özellikleri.). Sakarya Univ J Sci 21(2):190–202. https://doi.org/10.16984/saufenbilder.297005

Demirtaş M (2017b) High impact heat waves over the Euro-Mediterranean Region and Turkey—in concert with atmospheric blocking and large dynamical and physical anomalies. Anadolu Univ J Sci Technol A App Sci and Eng 18(1):97–114. https://doi.org/10.18038/aubtda.300426

Demirtaş M (2018) The high-impact 2007 hot summer over Turkey: atmospheric-blocking and heat-wave episodes. Meteorologic Appl 25(3):406–413. https://doi.org/10.1002/met.1708

Demirtaş M (2022) The anomalously cold January 2017 in the south-eastern Europe in a warming climate. Int J Climatol 1–9. https://doi.org/10.1002/joc.7574

Di Capua G, Sparrow S, Kornhuber K, Rousi E, Osprey S, Wallom D, van den Hurk B, Coumou D (2021) Drivers behind the summer 2010 wave train leading to Russian heatwave and Pakistan flooding. Clim Atmos Sci 4:55. https://doi.org/10.1038/s41612-021-00211-9

Domeisen DIV, Eltahir EAB, Fischer EM et al (2023) Prediction and projection of heatwaves. Nat Rev Earth Environ 4:36–50. https://doi.org/10.1038/s43017-022-00371-z

Feudale L, Shukla J (2007) Role of Mediterranean SST in enhancing the European heat wave of summer 2003. Geophys Res Lett 34:L03811

Feudale L, Shukla J (2011) Influence of sea surface temperature on the European heat wave of 2003 summer, part II: a modelling study. Climate Dynam 36:1705–1715

García-León D, Casanueva A, Standardi G et al (2021) Current and projected regional economic impacts of heatwaves in Europe. Nat Commun 12:5807. https://doi.org/10.1038/s41467-021-26050-z

Hersbach H, Bell B, Berrisford P, Hirahara S, Horanyi A, Muñoz-Sabater J, Nicolas J, Peubey C, Radu R, Schepers D, Simmons A, Soci C, Abdalla S, Abellan X, Balsamo G, Bechtold P, Biavati G, Bidlot J, Bonavita M et al (2020) The ERA5 global reanalysis. Q J Roy Meteorol Soc 146:1999–2049. https://doi.org/10.1002/qj.3803

Hochman A, Alpert P, Negev M, Abdeen Z, Mohsen A, Pinto JG, Levine H (2020) The relationship between cyclonic weather regimes and seasonal Influenza over the eastern Mediterranean. Sci Total Environ. https://doi.org/10.1016/j.scitotenv.2020.141686

Ionita M, Caldarescu DE, Nagavciuc V (2021) Compound hot and dry events in Europe: variability and large-scale drivers. Front Clim. https://doi.org/10.3389/fclim.2021.688991

Joint Research Centre - JRC (2021) "EU 2021 wildfire season was the second worst on record, finds new Commission report." https://joint-research-centre.ec.europa.eu/jrc-news/eu-2021-wildfire-season-was-second-worst-record-finds-new-commission-report-2022-03-21_en

Lenggenhager S, Martius O (2019) Atmospheric blocks modulate the odds of heavy precipitation events in Europe. Climate Dynam 53:4155–4171. https://doi.org/10.1007/s00382-019-04779-0

Mbokodo I, Bopape M-J, Chikoore H, Engelbrecht F, Nethengwe N (2020) Heatwaves in the future warmer climate of South Africa. Atmosphere. 11(7):712. https://doi.org/10.3390/atmos11070712

Pfahl S (2014) Characterising the relationship between weather extremes in Europe and synoptic circulation features. Nat Hazards Earth Syst Sci 14:1461–1475

Pfahl S, Wernli H (2012) Quantifying the relevance of atmospheric blocking for co-located temperature extremes in the Northern Hemisphere on (sub-)daily time scales. Geophys Res Lett 39(12). https://doi.org/10.1029/2012GL052261

Quandt LA, Keller JH, Martius O, Jones SC (2017) Forecast variability of the blocking system over Russia in summer 2010 and its impact on surface conditions. Weather Forecast 32:61–82. https://doi.org/10.1175/WAF-D-16-0065.1

Rex D (1950) Blocking action in the middle troposphere and its effect upon regional climate: I. An aerological study of blocking action. Tellus 2:196–211

Rodrigues RR, Taschetto AS, Gupta AS, Foltz GR (2019) Common cause for severe droughts in South America and marine heatwaves in the South Atlantic. Nat Geosci 12:620–626. https://doi.org/10.1038/s41561-019-0393-8

Sabah (2021) Turkey marks 10th day of forest fires with hopes of recovery Turkey marks 10th day of forest fires with hopes of recovery. https://www.dailysabah.com/turkey/turkey-marks-10th-day-of-forest-fires-with-hopes-of-recovery/news. (Accessed 25 January 2023)

Schaller et al (2018) Influence of blocking on Northern European and Western Russian heatwaves in large climate model ensembles. Environ Res Lett 13:054015. https://doi.org/10.1088/1748-9326/aaba55

Scherrer SC, Croci-Maspoli M, Schwierz C, Appenzeller C (2006) Two-dimensional indices of atmospheric blocking and their statistical relationship with winter climate patterns in the Euro-Atlantic Region. Int J Climatol 26:233–50

Schwierz C, Croci-Maspoli M, Davies HC (2004) Perspicacious indicators of atmospheric blocking. Geophys Res Lett 31:L06125. https://doi.org/10.1029/2003GL019341

The Telegraph (2021) Three dead and ten stranded as wildfire rages across southern Turkey. https://www.telegraph.co.uk/world-news/2021/07/29/one-dead-ten-stranded-wildfire-rages-across-southern-turkey/ (Accessed 25 January 2023)

Tibaldi S, Molteni F (1990) On the operational predictability of blocking. Tellus-A 42:343–365

Webber CP, Dacre HF, Collins WJ, Masato G (2017) The dynamical impact of Rossby wave breaking upon UK PM10 concentration. Atmospheric Chem Phys 17:867–881. https://doi.org/10.5194/acp-17-867-2017

World Meteorological Organization (WMO) (2022) https://public.wmo.int/en/media/press-release/2021-one-of-seven-warmest-years-record-wmo-consolidated-data-shows (Accessed 4 April 2022)

Xoplaki E, Gonzalez-Rouco JF, Luterbacher J, Wanner H (2003) Mediterranean summer air temperature variability and its connection to the large-scale atmospheric circulation and sea surface temperatures. Climate Dynam 20:723–739. https://doi.org/10.1007/s00382-003-0304-x

Zittis G, Hadjinicolaou P, Almazroui M et al (2021) Business-as-usual will lead to super and ultra-extreme heatwaves in the Middle East and North Africa. Climate and Atmospheric. Science 4(20). https://doi.org/10.1038/s41612-021-00178-7